Phys Chem Minerals (2001) 28: 706–710

ORIGINAL PAPER

H. Nagasawa · T. Suzuki · M. Ito · M. Morioka

Diffusion in single crystal of melilite: interdiffusion of Al + Al vs. Mg + Si

Received: 10 November 2000 / Accepted: 27 July 2001

Abstract Interdiffusion coefficients of Al + Al vs. Mg + Si in the gehlenite–åkermanite system of melilite were determined by coupled annealing of synthesized end-member single crystals. The observed diffusion coefficients for a couple-annealed sample vary for about 2 orders of magnitude, showing strong dependence on the gehlenite–åkermanite composition: diffusion coefficient observed at 1350 °C, for example, is 3×10^{-13} cm^2 s^{-1} at 5 mol% åkermanite composition (Ak_5), increases to 2×10^{-11} cm^2 s^{-1} at Ak_{80}, and then decreases to 1×10^{-12} cm^2 s^{-1} at Ak_{95}. The diffusion coefficient–temperature relation indicates high activation energy of diffusion of about 420 kJ mol^{-1} for gehlenite-rich melilite. The observed diffusion coefficient–composition relation may be explained by a combination of (1) the diffusion coefficient–melting temperature relation (Flynn's rule) and (2) the feasibility of local charge compensation, which can possibly be maintained more easily in the intermediate chemical composition. The high activation energy value for gehlenitic melilite appears to correspond to the complex diffusion mechanism. The observed highly variable diffusion coefficients suggest that gehlenite–åkermanite zoning in the melilite crystals in Ca, Al-rich inclusions in the carbonaceous meteorites may provide a sensitive indicator for the thermal history of the inclusions.

Key words Interdiffusion · Melilite · Åkermanite · Gehlenite

H. Nagasawa (✉) · T. Suzuki · M. Ito
Department of Chemistry,
Gakushuin University, Mejiro,
Toshima-ku, Tokyo 171-8588
e-mail: 620084@gakushuin.ac.jp

M. Morioka
Radio-isotope Centre,
University of Tokyo, Yayoi, Bunkyo-ku,
Tokyo 113-0032

Introduction

Melilite is a major constituent mineral in the Ca, Al-rich inclusions (CAIs) in the primitive chondrites, some of the earliest materials in the solar system. The melilite system in the CAIs is a solid solution of two end members, gehlenite ($Ca_2Al_2SiO_7$) and åkermanite ($Ca_2MgSi_2O_7$). Melilite crystals in CAIs are normally zoned or heterogeneous in terms of end-member compositions (e.g., Grossman 1975). The observed compositional zoning in the individual melilite grains must have been produced originally by fractional crystallization from Ca, Al-rich liquids (MacPherson et al. 1989), but might have been disturbed by diffusion during the cooling stages or later heating events (Grossman et al. 1977). Recent observation of heterogeneous oxygen isotope distribution within a single melilite grain in an Allende CAI suggests that the CAI was produced by a multiple heating event (Yurimoto et al. 1998). Thus, the interdiffusivities of gehlenite and åkermanite components in the melilite solid solution system are necessary to discuss the origin of CAIs, and may possibly provide an important clue to assess the formation processes of CAIs.

In a previous paper (Morioka and Nagasawa 1991), we reported the preliminary results of gehlenite–åkermanite interdiffusivities along the *c* axis which were measured using synthetic end-member single crystals by the diffusion couple technique (e.g., Elphic et al. 1985; Chakraborty and Ganguly 1992). The results showed that the diffusivities are strongly dependent on composition and, on average, considerably lower than those for most other cations in the melilite solid solution system measured by tracer techniques and pair annealing techniques (Morioka and Nagasawa 1991; Morioka et al. 1997). However, because of the low diffusivities, particularly along the *c* axis, and also because of the strong dependence of diffusivities on the concentration, the values determined for diffusion coefficient were subjected to considerably large uncertainties.

Couple annealing of gehlenite and åkermanite must accompany paired interdiffusion of $Al^{3+} + Al^{3+}$ vs. $Mg^{2+} + Si^{4+}$ since charge balancing is required to maintain solid solution. In the melilite structure, Al^{3+} ions occupy either T1 or T2 sites, while Mg^{2+} and Si^{4+} ions occupy T1 and T2 sites, respectively (Louisnathan 1971). Interdiffusion of ions under such complex conditions has not been well studied. Similar paired interdiffusion must also occur in some major rock-forming minerals, $Na^{+} + Si^{4+}$ vs. $Ca^{2+} + Al^{3+}$ in plagioclase, for example, in the terrestrial rock-forming processes. However, the mechanism of such paired interdiffusion, as well as the microdistribution of ions in the solid solution, has not been well understood.

In this paper we report the results of a gehlenite–åkermanite interdiffusion experiment performed along the *a* axis, which is about an order of magnitude larger than those along *c* axis, and discuss possible mechanisms for paired interdiffusion and some possible cosmochemical implications.

Experimental

Experimental procedures employed in this study are essentially similar to those in Morioka and Nagasawa (1991). Single crystals of gehlnite and åkermanite were synthesized with the Czochralsky pulling method from the starting material prepared by mixing reagent grade (3N) $CaCO_3$, Al_2O_3 and SiO_2, and $CaCO_3$, MgO, and SiO_2, respectively. Both end-member single crystals were cut into rectangular prisms with a polished *a* surface of about 2 × 3 mm and a thickness of about 2 mm. A pair of the end-member specimens was bound together by Pt wire with the polished *a* surface in contact with each other for coupled annealing. The coupled specimens were heated to 1200–1350 °C for 3–40 days. After diffusion annealing, the coupled specimens were cut parallel to the *a* axis and polished for microprobe analysis. Diffusion profiles were determined using a Hitachi S-2400 electron microscope equipped with a Horiba E-Max 7000 EDX (energy-dispersive X-ray analyzer) system.

Diffusion coefficients, $D(c')$, which are dependent on concentration, were calculated by PC-aided graphical fitting using the Boltzmann–Matano equation:

$$D(c') = (\mathrm{d}x/\mathrm{d}c)_{c'}/(2t)\int_0^{c'} x\,\mathrm{d}c \ , \qquad (1)$$

where c is the molar concentration of an end-member component, x is the distance from the Boltzmann–Matano interface which is the theoretically determined boundary between the two end-member crystals, t is the annealing time interval, and $D(c')$ is the diffusion coefficient at concentration c'.

Results

Results are listed in Table 1 and a diffusion profile obtained for the specimen annealed at 1350 °C for 3 days is shown in Fig. 1. Diffusion profiles determined for different annealing conditions show similar characteristic pattern with steep inclinations at both ends and a long plateau at the center, which confirms the preliminary

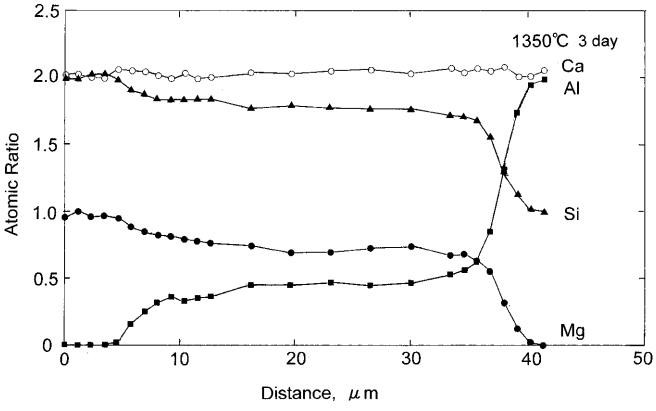

Fig. 1 Diffusion profile of a sample annealed at 1350 °C for 3 days

Table 1 Diffusion coefficients ($cm^2\ s^{-1}$) vs. composition

	T (°C)	1200	1250	1300	1300	1300	1350	1350	1350	1350	1350	1350	Δ*E*
	Time (day)	32	5	30	2	Average	5	5	3	3	3	Average	(kJ mol^{-1})
Gehlenite %	95	6.1E−15	4.1E−14	7.6E−14	1.0E−13	8.8E−14	9.3E−14	1.9E−13	8.9E−14	2.2E−13	1.4E−13	1.4E−13	410 ± 90
	90	7.4E−15	3.7E−14	8.0E−14	1.2E−13	1.0E−13	1.5E−13	1.9E−13	9.5E−14	2.6E−13	1.9E−13	1.7E−13	410 ± 60
	85	8.7E−15	3.9E−14	1.0E−13	1.3E−13	1.2E−13	2.0E−13	2.1E−13	1.2E−13	3.1E−13	2.2E−13	2.0E−13	420 ± 50
	80	9.9E−15	4.2E−14	9.6E−14	1.5E−13	1.2E−13	2.4E−13	2.2E−13	1.4E−13	4.3E−13	2.7E−13	2.4E−13	420 ± 40
	75	1.1E−14	4.4E−14	1.2E−13	1.6E−13	1.4E−13	2.6E−13	2.3E−13	1.5E−13	5.3E−13	3.1E−13	2.7E−13	430 ± 40
	70	1.3E−14	4.8E−14	1.4E−13	1.8E−13	1.6E−13	2.8E−13	2.6E−13	1.5E−13	6.6E−13	3.4E−13	3.0E−13	420 ± 40
	65	1.5E−14	5.4E−14	1.7E−13	2.0E−13	1.9E−13	3.1E−13	3.1E−13	1.6E−13	7.9E−13	3.9E−13	3.4E−13	420 ± 40
	60	1.8E−14	5.8E−14	2.0E−13	2.3E−13	2.2E−13	3.4E−13	3.5E−13	1.8E−13	9.4E−13	4.6E−13	3.9E−13	420 ± 40
	55	2.3E−14	6.3E−14	2.4E−13	2.7E−13	2.6E−13	4.1E−13	4.0E−13	2.0E−13	1.1E−12	5.3E−13	4.6E−13	410 ± 40
	50	3.1E−14	6.8E−14	2.9E−13	3.2E−13	3.1E−13	4.5E−13	4.9E−13	2.5E−13	1.4E−12	6.4E−13	5.4E−13	400 ± 50
	45	4.3E−14	7.0E−14	4.2E−13	4.2E−13	4.2E−13	5.0E−13	6.0E−13	2.8E−13	1.7E−12	7.7E−13	6.4E−13	390 ± 80
	40	4.4E−14	7.0E−14	5.9E−12	5.4E−13	3.2E−12	6.5E−13	8.0E−13	3.5E−13	2.4E−12	1.1E−12	8.6E−13	510 ± 260
	35	5.2E−14	6.9E−14	1.8E−12	8.4E−13	1.3E−12	9.8E−13	1.2E−12	4.5E−13	3.1E−12	1.6E−12	1.2E−12	490 ± 160
	30	6.2E−14	6.7E−14	7.5E−12	1.2E−12	4.4E−12	7.7E−12	2.8E−12	7.2E−13	8.0E−12	2.9E−12	3.3E−12	640 ± 240
	25	4.8E−14	6.5E−14	5.9E−12	1.8E−12	3.9E−12	3.1E−11	8.9E−12	1.2E−12	2.8E−11	1.2E−11	1.0E−11	800 ± 200
	20	4.2E−14	6.4E−14	4.6E−12	1.0E−12	2.8E−12	1.8E−11	1.1E−11	4.0E−12	4.0E−11	1.7E−11	1.4E−11	840 ± 180
	15	5.4E−14	6.8E−14	1.8E−12	1.0E−12	1.4E−12	4.3E−12	4.6E−12	1.2E−11	3.1E−11	7.2E−12	8.8E−12	720 ± 160
	10	4.6E−14	7.4E−14	6.4E−13	8.5E−13	7.5E−13	1.6E−12	1.8E−12	1.9E−12	8.4E−12	2.2E−12	2.5E−12	560 ± 100
	5	2.8E−14	7.5E−14	6.4E−13	6.7E−13	6.6E−13	7.2E−13	8.9E−13	5.2E−13	3.3E−12	1.2E−12	1.0E−12	500 ± 90

Overall uncertainties for *D* values are believed to be 30–40% for the gehlenite-rich side of composition, and higher for the åkermanite-rich side of composition

results of Al + Al vs. Mg + Si interdiffusion reported in Morioka and Nagasawa (1991). The observed diffusion profile indicates that the diffusion coefficient (D) is strongly dependent on composition, i.e., D is high in the intermediate composition and decreases rapidly towards the end-member compositions. In calculating Ds, each diffusion profile was smoothed and then Ds were calculated at 19 points at every 5% of Ge–Ak composition in each diffusion profile using Eq. (1). The values of D were determined by averaging the values obtained from the Al, Mg, and Si profiles. These three values deviate by 20–40%in the high-gehlenite side and 20–60% in the high-åkermanite side of the composition. The results of several repeated line analyses at the different positions at the boundary were averaged to determine the D values for a single run. Considering all sources of errors, the overall uncertainty level of the calculated values of D is believed to be 30∼40% at the high-gehlenite side of composition and higher at the high-åkermanite side of composition. In Fig. 2, Ds thus obtained at 1350 °C are plotted.

Spatial resolution of the EDX measurement is approximately 1–2 μm, which may be insufficient for accurate determination of low D values at the diffusion front. However, since the observed points in the diffusion profiles continue smoothly from a high D portion in the intermediate composition to the low D ends towards the terminal compositions, spatial resolution does not significantly affect the conclusion of the present work.

Discussion

Scatter of the results for different runs

As is shown in Table 1 and Fig. 1, the values observed for different runs scatter considerably. One of the reasons for the scatter is difficulty in fitting the observed diffusion profile to Eq. (1). Because of the strong dependence of D on composition, one particular heating duration can be too short for sufficient diffusion in the low D part of the profile, while it is adequate or even too long for the high D part of the profile. In addition, adequate heating duration for observing the low D part of the diffusion profile can be inconvenient for practical reasons. Heating for months or years is impractical, and even if the long heating duration was applied, it becomes more plausible that cracks or imperfections are introduced to the diffusion area to interfere observation of diffusion profiles.

Another possible cause for the scatter may be in the behavior of the melilite solid solution. We have aligned two end-member crystals by eye observation for coupled annealing. Therefore, the crystal axis is not well aligned in terms of the atomic scale. Nevertheless, the two end-member crystals were welded together very well during

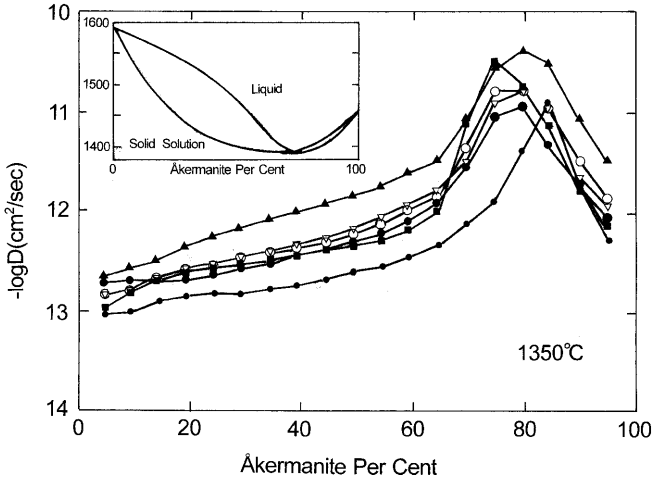

Fig. 2 Diffusion coefficient vs. composition relation for the samples annealed at 1350 °C. *Open circles* indicate the average values. The observed relation shows maximum at about the composition with minimum melting temperature, which is shown in the phase diagram of the Gh–Åk system *inserted* in the figure (Osborn and Schairer 1941)

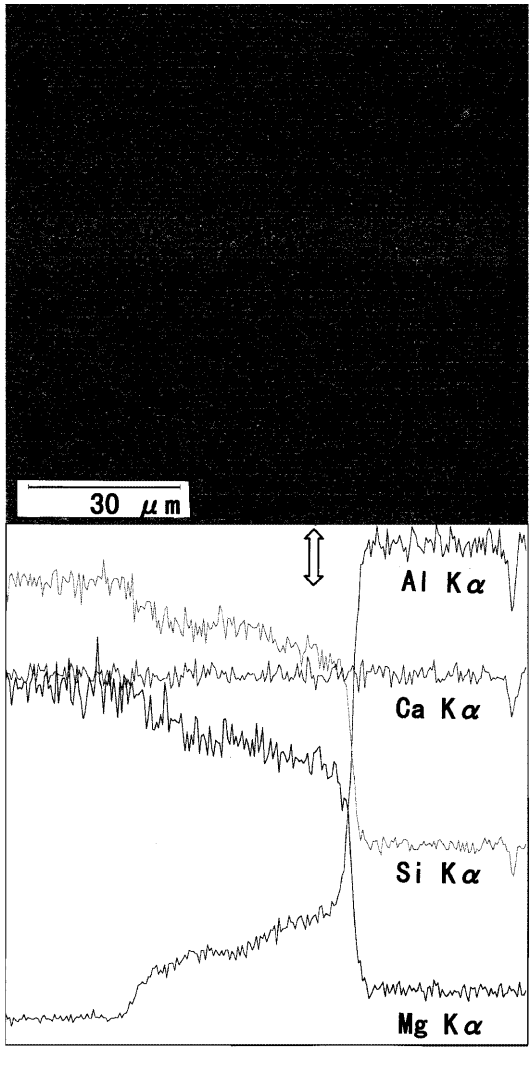

Fig. 3 A SEM image and X-ray line profiles of an annealed sample at the Gh–Åk interface. Note that the boundary between the two end-member crystals is fused together very well so that the original boundary (approximate position of the Boltzmann–Matano interface is shown by the *arrow*) cannot be seen in the image

diffusion annealing, as shown in the electron micrograph (Fig. 3), suggesting the adjustment of the crystal lattice occurred at the interface of both crystals during annealing. In the case of coupled annealing of olivine end members (Morioka 1980, 1981), forsterite and Co-olivine for example, it is observed that the position of the original boundary of the end-member crystals can clearly be identified as the lines of spots or voids, etc. under electron microscopic observation. In the case of annealing olivine crystals, adjustment of crystal lattice appears to occur only locally, and thus mismatching of crystal lattices remains as spots or voids at the boundary. If fairly long-scaled adjustment of the crystal lattice occurred at the interface of the melilite end members, then diffusion mixing can be affected by an insufficient alignment of the crystal lattice. Insufficient alignment would produce a coherency strain that contributes the production of vacancies, dislocations, etc. (e.g., Sutton and Balluffi 1996) that would enhance the diffusivities of cations. Thus, the insufficient alignment of paired crystals can be one of the reasons for the observed scatter of D. However, this does not necessarily mean that insufficient alignment is the major reason for the observed high D or the plateau in the diffusion profile at the intermediate composition, as discussed in the next section.

Diffusion mechanisms

As discussed in the previous section, two end-member crystals were welded together so well by diffusion annealing that the position of the original boundary is not clearly seen in the electron micrograph. The observed continuum at the boundary suggests formation of solid solution with continuous composition change, and thus interdiffusion of Al + Al vs. Mg + Si occurred continuously and smoothly.

As shown in Fig. 2, D shows a maximum at about Ak_{80}, which approximately corresponds to the composition ($Ak_{\sim 75}$) of the lowest melting temperature (ca. 1370 °C) in the phase diagram of the gehlenite–åkermanite system (Osborn and Schairer 1941). The observed relationship between D and melting temperature is consistent with that generally observed for alloys (Flynn's rule: Flynn 1972; Morioka and Nagasawa 1991). However, since the calculated D values vary so widely, by about 2 orders of magnitude, it is difficult to judge if the observed relation between D and composition can be explained only by Flynn's rule.

Difficulty in charge balancing through movement of paired ions near terminal compositions may be another explanation for the steep decrease of D observed at both ends of the diffusion profile. Diffusion of paired ions requires the condition that pairing ions must be in near-by sites for charge compensation. At the diffusion front, the lower probability of finding paired ions in near-by sites would reduce the diffusivity of paired ions.

Diffusivity of Mg and Si into the gehlenite lattice observed at the diffusion front is considerably lower than that of two Al ions into the åkermanite lattice. The observed lower diffusivity of Mg and Si can be explained phenomenologically by Flynn's rule, i.e., the higher melting temperature of gehlenite tends to reduce diffusivities of cations compared with the lower melting temperature of åkermanite.

However, an alternative explanation is possible. In åkermanite Mg and Si occupy T2 and T1 sites, respectively, while in gehlenite Al occupies either T1 and T2 sites. At the diffusion front, diffusion paths of Mg and Si are limited to T1 to T1 and T2 to T2, respectively. Al ions, on the other hand, have more freedom on diffusion paths, since Al ions can diffuse through either T1 and T2 sites.

Insufficient alignment of two end-member crystals, as discussed in the previous section, may produce distortion, defects, and/or dislocations in the crystal at the interface of the two crystals, and thus enhance diffusion mixing of two end-member components. This may contribute to the high diffusivities observed at the intermediate compositions. However, the maximum in the diffusion coefficient vs. composition relation observed at the composition of $Ak_{\sim 80}$, which is corresponding approximately to the lowest melting temperature of the solid solution system, cannot be explained by this effect. Furthermore, high diffusivity in the intermediate composition was not observed for other systems, such as åkermanite–Co–åkermanite interdiffusion experiments (Morioka and Nagasawa 1991) in which insufficient alignment of crystal lattices must have occurred in similar degrees. Thus, this effect of insufficient alignment of two end-member crystal lattices cannot be the major reason for the high diffusion coefficients at the intermediate composition.

Log D vs. temperature relations are plotted in Fig. 4. The estimated values of activation energy of diffusion are 410–430 kJ mol^{-1} for Ak-poor composition with statistical errors of about 10–20%. These values are

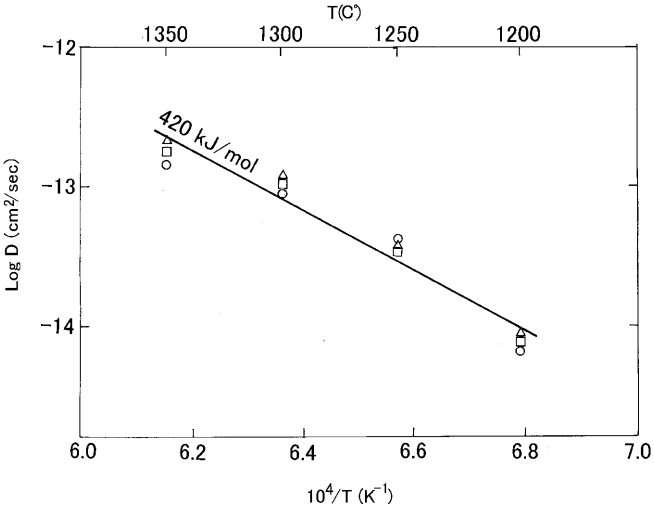

Fig. 4 Arrhenius plot for Gh_{95} (△), Gh_{90} (□) and Gh_{85} (○). *Broken line* indicates reference line for activation energy of 420 kJ mol^{-1}

significantly higher than those for diffusion of intermediate-sized divalent cations in åkermanite (Morioka and Nagasawa 1991; Morioka et al. 1997) and close to the values for Ni diffusion in gehlenite, in which substitution of Ni for Al in T1 site requires some kind of charge compensation. Although the activation energy values observed in this study may be subjected to even higher uncertainties due to the technical difficulty in determining diffusion coefficient values, etc., the higher activation energies appear to be real, since activation energy values are even higher at the Ak-rich side of composition (the calculated values of activation energies for different compositions are tabulated in Fig. 1). The calculated higher activation energies may indicate that the mechanism of such interdiffusion of ion pairs which requires charge compensation is more complicated than that for interdiffusion of single-cation species in åkermanite.

Possible implications

Heterogeneous distribution of oxygen isotopes within a single CAI observed by Yurimoto et al. (1998) implies that CAIs were produced by multiple heating events in the early solar system, some 4.5×10^9 years ago. Furthermore, it is observed that oxygen isotope ratios change from normal to anomalous within a 10-micron scale, so that the heating event lasted for very short time interval and thus did not affect the distribution of oxygen isotopes in a 10-micron scale by diffusion.

Diffusion coefficients of oxygen in silicate are substantially lower than those of cations in the same mineral in most silicates (e.g., Yurimoto et al. 1989). Based on the higher diffusivities, distributions of cations in CAIs can be more sensitive indicators of thermal events of short time intervals. However, minerals in CAIs are composed exclusively of refractory elements, and thus the choice of cations for a sensitive indicator for thermal events is very limited. The observed interdiffusivities of gehlenite–åkermanite components suggest a possible applicability to the wide range of heating intervals, since the observed diffusion coefficients vary for about 2 orders of magnitude, depending on the gehlenite–åkermanite composition.

The average compositions of melilite for type A and B CAI are Ak_{18} and Ak_{30}, respectively, and usually vary widely within a CAI and even in a single crystal from almost pure gehlenite up to about Ak_{75}. Ak_{75} corresponds approximately to the composition with highest diffusivity. The high åkermanite composition which is still remaining in the melilite in the CAIs suggests an even shorter time interval of heating of the CAIs compared with that estimated from the distribution of oxygen isotope anomalies. For this purpose, careful measurement of Ge–Ak zoning together with the determination of distribution of oxygen isotopes anomalies should be necessary.

Acknowledgements We thank J. Ganguly and O. Jaoul for their kind and constructive suggestions and reviews. We also thank Y. Inaguma for helpful discussions. This work is partly supported by the Grant-in-Aid from the Ministry of Education, No. 09440193.

References

Chakraborty S, Ganguly J (1992) Cation diffusion in aluminosilicate garnets: experimental determination in spessartine–almandine diffusion couples, evaluation of effective binary diffusion coefficients, and applications. Contrib Mineral Petrol 111: 74–86

Elpick SC, Ganguly J, Loomis TP (1985) Experimental determination of cation diffusivities in aluminosilicate garnets. I. Experimental methods and interdiffusion data. Contrib Mineral Petrol 90: 36–44

Flynn CP (1972) Point defects and diffusion. Clarendon Press, p 826

Grossman L (1975) Petrography and mineral chemistry of Ca-rich inclusions in the Allende meteorite. Geochim Cosmochim Acta 39: 433–453

Grossman L, Ganapathy R, Davis AM (1977) Trace elements in the Allende meteorite III. Coarse-grained inclusions revisited. Geochim Cosmochim Acta 41: 1647–1664

Louisnathan SJ (1971) Refinement of the crystal structure of a natural gehlenite, $Ca_2Al(Al,Si)_2\ O_7$. Can Mineral 10: 822–837

MacPherson GJ, Crozaz G, Lindberg LL (1989) The evolution of a complex type B Allende inclusion: an ion microprobe trace element study. Geochim Cosmochim Acta 53: 2413–2427

Morioka M (1980) Cation diffusion in olivine I. Cobalt and magnesium. Geochim Cosmochim Acta 44: 759–762

Morioka M (1981) Cation diffusion in olivine II. Ni–Mg, Mn–Mg, Mg and Ca. Geochim Cosmochim Acta 45: 1573–1580

Morioka M, Nagasawa H (1991) Diffusion in single crystals of melilite II. Cations. Geochim Cosmochim Acta 55: 751–759

Morioka M, Kamata Y, Nagasawa H (1997) Diffusion in single crystals of melilite III. Divalent cations in gehlenite. Geochim Cosmochim Acta 61: 1009–1016

Osborn EF, Schairer JF (1941) The ternary system pseudowollastonite–akermanite–gehlenite. Am J Sci 239: 715–763

Sutton AP, Balluffi (1996) Coherency interfacial dislocations. In: Interfaces in crystalline materials. Clarendon Press, Oxford, p 81

Yurimoto H, Morioka M, Nagasawa H (1989) Diffusion in single crystals of melilite I. Oxygen. Geochim Cosmochim Acta 53: 2387–239

Yurimoto H, Ito M, Nagasawa H (1998) Oxygen isotope exchange between refractory inclusions in Allende and solar nebular gas. Science 282: 1874–1877